New Phytologist

In vivo assessment by Mach–Zehnder double-beam interferometry of the invasive force exerted by the Asian soybean rust fungus (*Phakopsora pachyrhizi*)

Marco Loehrer[1], Jens Botterweck[1], Joachim Jahnke[2], Daniel M. Mahlmann[3], Jochem Gaetgens[4], Marco Oldiges[4], Ralf Horbach[5], Holger Deising[5,6] and Ulrich Schaffrath[1]

[1]Department of Plant Physiology, RWTH Aachen University, D-52056 Aachen, Germany; [2]Department of Soil Ecology, RWTH Aachen University, D-52056 Aachen, Germany; [3]Technology of Optical Systems (TOC), RWTH Aachen University, D-52056 Aachen, Germany; [4]Institute of Bio- and Geosciences: IBG-1 Biotechnology, Forschungszentrum Jülich GmbH, 52425 Jülich, Germany; [5]Interdisciplinary Centre for Crop Plant Research (IZN), Martin-Luther-University Halle-Wittenberg, D-06120 Halle (Saale), Germany; [6]Institute of Agricultural and Nutritional Sciences, Phytopathology and Plant Protection, Martin-Luther-University Halle-Wittenberg, D-06120 Halle (Saale), Germany

Author for correspondence:
Ulrich Schaffrath
Tel: +49 241 8020100
Email: schaffrath@bio3.rwth-aachen.de

Received: *25 October 2013*
Accepted: *24 February 2014*

New Phytologist (2014) **203:** 620–631
doi: 10.1111/nph.12784

Key words: appressorial turgor pressure, Asian soybean rust (*Phakopsora pachyrhizi*), cytorrhysis, interferometry, melanin, penetration by force, sugar alcohols.

Summary

• Asian soybean rust (*Phakopsora pachyrhizi*) causes a devastating disease in soybean (*Glycine max*). We tested the hypothesis that the fungus generates high turgor pressure in its hyaline appressoria to mechanically pierce epidermal cells.

• Turgor pressure was determined by a microscopic technique, called transmitted light double-beam interference Mach–Zehnder microscopy (MZM), which was developed in the 1960s as a forefront of live cell imaging. We revitalized some original microscopes and equipped them for modern image capturing. MZM data were corroborated by cytorrhysis experiments.

• Incipient cytorrhysis determined the turgor pressure in appressoria of *P. pachyrhizi* to be equivalent to 5.13 MPa. MZM data revealed that osmotically active sugar alcohols only accounted for 75% of this value. Despite having a lower turgor pressure, hyaline rust appressoria were able to penetrate non-biodegradable polytetrafluoroethylene (PTFE) membranes more efficiently than do melanized appressoria of the anthracnose fungus *Colletotrichum graminicola* or the rice blast fungus *Magnaporthe oryzae*.

• Our findings challenge the hypotheses that force-based penetration is a specific hallmark of fungi differentiating melanized appressoria and that this turgor-driven process is solely caused by metabolic degradation products. The appressorial turgor pressure may explain the capability of *P. pachyrhizi* to forcefully invade a wide range of different plants and may pave the way to novel plant protection approaches.

Introduction

Asian soybean rust (ASR), caused by the fungal plant pathogen *Phakopsora pachyrhizi*, is one of the most destructive diseases in soybean (*Glycine max*) worldwide, and has the potential to cause total loss of harvest (Goellner *et al.*, 2010). Cultivars with resistance to all known races of the fungus are unknown, and this leaves farmers with only the option of spraying fungicides, which is cost intensive and may cause environmental problems (Loehrer & Schaffrath, 2011). The search for novel sources of ASR resistance, for example, by investigating the mechanisms of non-host resistance in *Arabidopsis thaliana*, has so far been unsuccessful (Loehrer *et al.*, 2008; Langenbach *et al.*, 2013). An alternative approach to control ASR may be to target essential virulence mechanisms in the infection process of *P. pachyrhizi*. However, although much is known about the general infection cycle of *P. pachyrhizi*, some fundamental aspects, for example, the mode of invasion of host cells, are still enigmatic. In this study, we applied Mach–Zehnder microscopy (MZM) to fungal infection structures. Using this non-invasive *in vivo* method, we were able to measure solute concentrations in single cells and to deduce the contribution of sugar alcohols to the force exerted by appressoria of *P. pachyrhizi* when penetrating its soybean host.

The basidiomycete *P. pachyrhizi* belongs to the rust fungi and is characterized by an obligate-biotrophic lifestyle, that is, it depends on living host tissue for feeding and completion of its life cycle. Epidemics rely solely on uredospore dispersal and no sexual reproduction has been reported so far. After landing on the host, uredospores germinate and the single germ tube differentiates a specialized cell, called an appressorium. Appressoria are common infection structures among plant pathogenic fungi and are involved in the penetration of either the intact plant surface or a natural opening, such as the stomatal pore (Deising *et al.*, 2000). In contrast with the vast majority of rust fungi which build their appressorium above stomata to invade the intercellular spaces of the mesophyll, thereby possibly circumventing

epidermal defence responses, *P. pachyrhizi* penetrates intact epidermal cells directly (Goellner *et al.*, 2010). It must be remembered, however, that basidiospores of heteroecious rusts are also able to penetrate their plant host directly (Freytag *et al.*, 1988). A further uncommon feature of the penetration process of *P. pachyrhizi* is the concomitant death of the first penetrated cell which is unexpected for a biotrophic pathogen (Loehrer *et al.*, 2008). Interestingly, successful penetration does not only occur on the host, but also on non-host plants, such as barley, *Medicago truncatula* and *A. thaliana* (Loehrer *et al.*, 2008; Hoefle *et al.*, 2009; Uppalapati *et al.*, 2012). Data from transgenic barley plants expressing the cell death suppressor BAX inhibitor-1 suggest that *P. pachyrhizi*, at least on barley, depends on this cell death to facilitate entry into epidermal tissue (Hoefle *et al.*, 2009). Subsequently, *P. pachyrhizi* forms haustorial mother cells in the intercellular space from which the pathogen starts to invade mesophyll cells by forming feeding cells, so-called haustoria. Further proliferation occurs throughout the host tissue, and differentiation into uredia which produce uredospores, completes the life cycle of this fungus (Goellner *et al.*, 2010).

In order to investigate the mechanism of the penetration by *P. pachyrhizi* of a wide range of different host plants, we investigated the involvement of turgor pressure in the penetration process. Basically, the interplay of cell walls and turgor pressure determines the mechanophysical properties of cells from plants, fungi and water moulds (chromista) (Geitmann, 2006). Fungi, in particular, utilize turgor pressure to drive hyphal extension and the penetration of hard surfaces (Money, 2004; Lew, 2011). For apical tip growth of fungal hyphae, a turgor pressure of 0.6 MPa is required (Money, 2004). In some specialized infection structures, such as appressoria, turgor pressure has been estimated to be approximately a magnitude higher (Howard *et al.*, 1991; de Jong *et al.*, 1997; Bechinger *et al.*, 1999). This enormous pressure is supposed to be translated into force required to mechanically breach a leaf surface and facilitate entry of a pathogen into its host (de Jong *et al.*, 1997; Bechinger *et al.*, 1999).

Transmission electron microscopy suggests that *P. pachyrhizi* requires the successive or concomitant application of mechanical force and cell wall-degrading enzymes to breach the cuticle and plant cell walls of its soybean host (Edwards & Bonde, 2011). However, no experimental data supporting force application by appressoria of *P. pachyrhizi* are as yet available. One way to address this question experimentally is to estimate appressorial turgor pressure through the measurement of incipient cytorrhysis, an assay in which the osmotic pressure (Π) of a cell is balanced with the osmotic potential (Ψ_Π) of the surrounding medium. Basically, when cells are placed in hypertonic solution, there are two possible outcomes: if the osmolyte can pass freely through the cell wall, plasmolysis occurs, that is, the protoplast retracts from the wall and rounds up. However, if the cell wall is impermeable to the osmolyte or if cell wall polymers are linked to the plasmamembrane via glycosylphosphatidyl inositol (GPI)-anchored proteins (Latgé, 2007), the whole structure buckles and deforms, a condition known as cytorrhysis. Another way to measure forces locally exerted by single appressoria was followed with *Colletotrichum graminicola* using elastic optical waveguides (Bechinger *et al.*, 1999). However, a limitation of this method is its restriction to fungi that form infection structures on optical waveguides.

The technique of MZM is a tool allowing the non-invasive visualization of phase shift phenomena in living cells (Fig. 1). The magnitude of these phase shifts varies depending on the composition or concentrations of different substances within a cell. The physical principle of interference microscopy is the splitting of a light beam into two coherent beams, one passing through a cell of interest and the reference beam solely traversing the surrounding medium (Fig. 1b; Mahlmann *et al.*, 2008). The analysis of both beams in a single image results in a phase shift or optical path difference (OPD), which can be visualized by interference band patterns that are superimposed on the specimen sample image (Fig. 1c) and which are converted to coloured areas in true interference contrast (Fig. 1d). The OPD is correlated directly with the dry mass content of the investigated cell. According to Mahlmann *et al.* (2008), the best adaptation of interference microscopy was achieved by the dual-beam interference microscope developed by Horn in 1958, combining the Mach–Zehnder interferometer with two optically identical, but independent, microscope optics in each beam pathway (Fig. 1a). For a long time, the potential of this powerful tool has not been recognized and, today, only a very limited number of these sophisticated microscopes are still available. Importantly, Mahlmann *et al.* (2008) developed a software-aided analysis tool that allows image processing with precise measurements at a single pixel level. This improvement was indispensable for the development of MZM, allowing accurate quantification of dry masses at the single cell level, which is applicable to many biological systems (Jahnke *et al.*, 2011). Our study clearly shows that MZM has the potential to become a standard method for the analysis of the turgor pressure of fungal infection cells.

In this study, we used incipient cytorrhysis to determine the turgor pressure of the appressoria of *P. pachyrhizi*. MZM data unravelled the contribution of osmolytically active sugar alcohols to the overall turgor pressure. The appressoria of *P. pachyrhizi* are not melanized as is the case for *Magnaporthe oryzae* and *C. graminicola*, two hemibiotrophic pathogens, which are known to generate high turgor pressure within their appressoria. Importantly, our results demonstrate that melanization is not required in appressoria for the generation or withstanding of high turgor pressure. Our data were supported by experiments with artificial non-biodegradable membranes of highly defined thickness that could be breached by appressoria of *P. pachyrhizi*, but not *M. oryzae*.

Materials and Methods

Fungal material

The Brazilian *P. pachyrhizi* isolate BR05 was maintained on the susceptible soybean (*G. max*) cultivar Monsoy 5826. Sixteen-day-old plants were spray inoculated using a uredospore suspension generated by rinsing a completely infected primary soybean leaf in 50 ml of distilled water containing 0.1% Tween-20. After

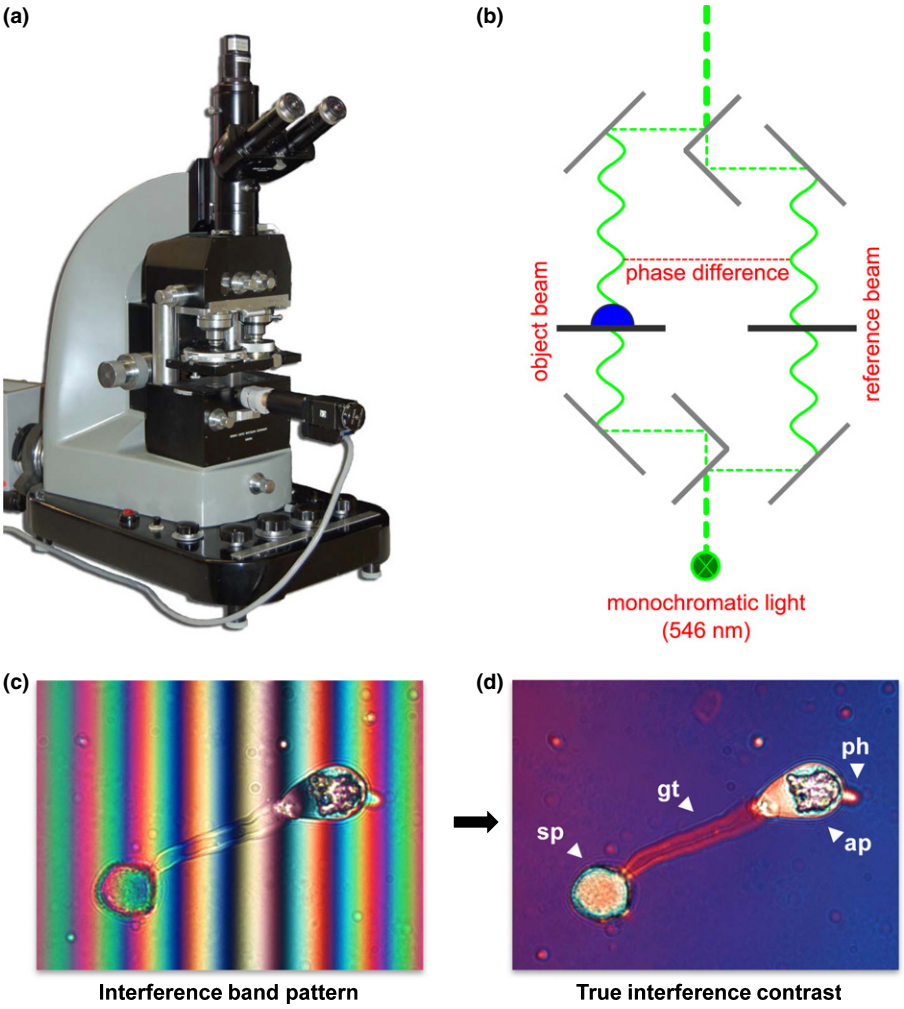

Fig. 1 Mach–Zehnder interferometry. The double-beam interference microscope manufactured by Leitz in 1960 was used in this study (a). This microscope consists of two separate optical paths which allow high-precision measurement of the phase shift caused by a microscopic object in the 'object beam' in comparison with an 'empty' sample in the 'reference beam' (b). Using interference microscopy, living cells, such as germinating uredospores of *Phakopsora pachyrhizi*, can be analysed without using reactive agents or dyes. The difference in phase (= OPD, 'optical path difference') is normally not perceivable with the human eye. Using this microscope, the phase shift is converted into contrast differences, which become visible as an 'interference band' pattern (c) or as coloured areas in true interference contrast (d). Images in (c) and (d) show the same *P. pachyrhizi* uredospore (sp) with a germ tube (gt), an appressorium (ap) and a penetration hypha (ph).

inoculation, plants were placed in the dark in a moist chamber (26°C and 100% relative air humidity) for 24 h. Afterwards, plants were transferred to a growth chamber (22°C, 60% relative air humidity and a photoperiod of 16 h at 306 µmol m^{-2} s^{-1}). Dry uredospores were harvested *c.* 10 d after inoculation by shaking the infected leaves. To obtain freshly produced *P. pachyrhizi* uredospores for the germination assay on glass slides, older uredospores were removed from the leaves by shaking 1 d before spore harvest. The *M. oryzae* isolate *TH6772* was cultivated and the spores were harvested as described in Zellerhoff *et al.* (2010). Before use, *M. oryzae* spores were washed three times in excess volumes of sterile double-distilled water to minimize traces of culture medium and contamination with the cytosol of broken hyphae.

GC-MS analyses of fungal infection structures

Uredospores of *P. pachyrhizi*, harvested from infected plants, and conidia of *M. oryzae*, collected from agar plates, were suspended in double-distilled water. After 1 h, each spore suspension was homogenized using five glass beads (1.7–2.1 µm) and a Precellys homogenizator (PEQLAB, Erlangen, Germany) and centrifuged for 20 min at 20 000 ***g***. The supernatants (500 µl) were used for further analyses. Fractions of germinated spores containing germ tubes and appressoria were generated by preparing the spore suspension as described above, followed by incubation at room temperature for 1 h, and plating the suspension in a thin water film on a glass slide before harvesting after 5 h (germ tubes) or 8 h (appressoria). The spore suspensions were collected from the glass slides and homogenization was carried out as described above. Before analysis, 13-µl aliquots of samples were lyophilized overnight and stored at −20°C. The dried samples were consecutively derivatized with 50 µl of MeOX (20 mg ml^{-1} *O*-methylhydroxylamine in pyridine) for 90 min at 30°C and 600 rpm in an Eppendorf thermomixer, followed by incubation with an additional 80 µl of MSTFA (*N*-acetyl-*N*-(trimethylsilyl)-trifluoroacetamide) for 90 min at 40°C and 600 rpm. For the determination of derivatized metabolites, an Agilent 6890N gas chromatograph (GC) (Agilent Technologies Inc., Santa Clara, CA, USA), coupled to a Waters Micromass GCT Premier high-resolution time-of-flight mass spectrometer (ToF-MS), was used. The system was controlled by Waters MassLynx 4.1 software (Waters Corp., Milford, MA, USA). Injection was performed by a Gerstel MPS 2 (Gerstel GmbH & Co. KG, Mülheim an der Ruhr, Germany) controlled by Maestro software. Samples (1 µl) were injected into a split/splitless injector at 280°C at varying split modes. The GC

was equipped with a 30-m Varian FactorFour VF-5ms + 10 m guard column (Agilent Technologies). A constant helium flow was set to 1 ml min^{-1}. The GC temperature program started at 60°C with a hold time of 2 min, followed by a temperature ramp of + 12°C min^{-1} to the final temperature of 300°C and a final hold time of 8 min (total run time, 30 min). The transfer line temperature was set to 300°C. The ToF-MS was operated in positive electron impact $[EI]^+$ mode at an electron energy of 70 eV with the source temperature set to 180°C. The MS was tuned and calibrated with the mass fragmentation pattern of heptacosafluoro-tributylamine. During analysis, the accurate masses were corrected to a single point lockmass of CPFB (chloro-pentafluoro-benzene) as an external reference at 2 019 609 *m/z*. Data acquisition was performed in centroid mode with a rate of 0.09 s per scan and an interscan delay of 0.01, i.e. 10 scans s^{-1}. For the identification of known metabolites, a baseline noise-subtracted fragment pattern was used in comparison with an in-house database (JuPoD), the National Institute of Standards and Technology (NIST) commercial database and the public domain Golm-Metabolome Database (GMD) (Hummel *et al.*, 2010). Unknown peaks were identified by structural combination of elemental compositions and verified by virtual derivatization and fragmentation of the predicted structure.

In vitro formation of infection structures and glycogen staining

Freshly harvested uredospores were suspended in distilled water (50 mg ml^{-1}) and incubated at room temperature for 2 h with gentle shaking. Germinated uredospores were thinly plated on glass slides using a micropipette tip with the terminal 2–3 mm removed to widen the aperture. The glass slides were placed in a moist chamber at 100% relative humidity. Germ tubes formed appressoria after 8 h on the glass slides. For the analysis of empty appressoria (after the formation of penetration hyphae), the uredospores were incubated for 24 h. Haematoxylin staining was performed directly on the microscopic slides immediately before observation. The staining solution was prepared according to Horobin & Murgatroyd (1971). The iodine–potassium iodide solution (5 g KI, 1.5 g I, 100 ml distilled water) for the staining of fungal structures was diluted 1 : 20 with distilled water before application. For comparison with *in vitro* experiments, fungal infection structures formed on the leaf surface of *G. max* were stained with aniline blue in lactic acid after clearing the leaves in a solution of ethanol and glacial acetic acid (6 : 1, v/v).

Mach–Zehnder double-beam interference microscopy

For analysis of the appressoria which were formed on the glass slides, cover glasses were put on the slides and sealed with nail varnish to reduce evaporation. The Mach–Zehnder transmitted light double-beam interference microscope (Mach-Zehnder Interference Microscope, Leica Microsystems, formerly Leitz, Wetzlar, Germany) required an additional microscope slide with water and a cover glass, but without fungal infection structures, as a reference. As described above, the OPD distribution was calculated by capturing a series of five images in interference contrast with a homogeneous background, shifted in phase for $\lambda/4$ each ($\lambda = 546$ nm), using dedicated software (Mahlmann *et al.*, 2008) based on an algorithm from Schwider *et al.* (1983). Measurements of the area and calculations of the volume were performed on the basis of transmission light micrographs and a stage micrometer. Volumes of appressoria for *P. pachyrhizi* and *M. oryzae* were estimated as spheres ($V = 4/3\pi r^3$) and spheroids ($V = 4/3\pi ab^2$), respectively. Mean values for the concentration of dry mass of fully turgid and empty appressoria were calculated using dn/dc (differential index of refraction) values of 0.145 for *P. pachyrhizi* and 0.135 for *M. oryzae* (Supporting Information Table S1b), which were based on the constituents of appressoria as determined by GC-MS. The constituents taken into account yielded 85% of the summed peak areas of all identified peaks. To calculate the concentration of cytosolic substances, the concentration of dry mass was divided by the mean molar mass of the identified substances and substituted in the van't Hoff equation ($\Pi = cRT$). *Magnaporthe oryzae* appressoria specimens for the measurement of the cell wall fraction ('empty app') were obtained by sonication of the sealed slides and thus disruption of the fully turgid appressoria.

Cytorrhysis experiments

Sorbitol solutions were generated by dissolving calculated amounts of sorbitol in distilled water. As the van't Hoff equation for the determination of the osmotic potential is only accurate for dilute solutions, we used a freezing point depression cryoscope (micro-osmometer; Knaur, Berlin, Germany) to determine the osmotic potential of these solutions. Appressoria of *P. pachyrhizi* formed on glass slides after 8 h (see earlier) were washed with the corresponding sorbitol solutions and incubated in these solutions for 15 min at room temperature. Appressoria of *M. oryzae* were used for cytorrhysis experiments 24 h after transferring spores onto glass slides. Infection structures were inspected by bright-field microscopy using a Leica DMRBE microscope (Leica Microsystems). Images were taken with a digital JVC KYF 750 (JVC Professional Europe Ltd, London, UK) camera.

Penetration of polytetrafluoroethylene (PTFE) membranes

PTFE membrane fabrication, including film deposition and extensive quality control, was performed as described by Kuster *et al.* (2008). Spores of *P. pachyrhizi* and *M. oryzae* were harvested as described above. At first, spores were germinated in double-distilled water supplemented with 0.01% (v/v) Tween-20 for 5–6 h at 23°C, and then transferred onto membranes. Spores of *C. graminicola* were handled as described in Ludwig *et al.* (2013). To dissolve the potassium bromide (KBr) layer underneath the PTFE-like membrane, sterile distilled water was pipetted along the edges of the glass slide to the point of membrane flotation. The membranes were incubated in sealed Petri dishes at 23°C for 48 h to allow appressorium differentiation and penetration. The success of the latter event was confirmed using a Nikon Eclipse E600 microscope (Nikon, Düsseldorf, Germany) equipped with bright field optics.

Results

Mobilization of cytosolic compounds during germination and appressorium formation

In order to determine appressorial osmolyte concentrations, we established an experimental set-up allowing the differentiation of *in vitro* infection structures on glass slides. Although the germination and formation of appressoria on glass slides have been described previously for *P. pachyrhizi* (Bromfield, 1984; Koch & Hoppe, 1988), we modified the procedure to promote the formation of penetration hyphae. Crucially, the volume needed to be small, so that spores germinated in close contact with the underlying glass surface in a moist chamber which prevented infection structures from desiccation. A comparative analysis with respect to timing and morphology of *in vitro* and *in vivo* germinated *P. pachyrhizi* uredospores revealed no substantial differences (Fig. S1), suggesting that no plant stimuli are required to initiate the development of infection structures.

Using this system, we analysed histochemically whether storage substances, such as glycogen, are mobilized during the germination of uredospores, applying iodine–potassium iodide or haematoxylin (Horobin & Murgatroyd, 1971; Thines *et al.*, 2000). Both staining methods revealed the presence of glycogen in uredospores before germination (Fig. 2a,g) and its partial relocation into germ tubes (Fig. 2b,c,h,i) and appressoria (Fig. 2d,j). At 8 h after germination, glycogen was not detectable by iodine–potassium iodide or haematoxylin in any of the infection structures (Fig. 2e,f,k,l). Glycogen was never detected in penetration hyphae, indicating a complete conversion of the polymer during the formation of appressoria.

Estimation of turgor pressure in appressoria by incipient cytorrhysis

Glycogen depletion during the maturation of appressoria of *P. pachyrhizi* was reminiscent of mobilization of glycogen rosettes in appressoria of *M. oryzae* (Thines *et al.*, 2000). These authors proposed that glycogen degradation products, such as glycerol, contribute almost exclusively to the generation of a high osmotic potential exceeding 8 MPa in appressoria of *M. oryzae*, which then allows the mechanical penetration of rice epidermal cells (Howard *et al.*, 1991; de Jong *et al.*, 1997). We applied incipient cytorrhysis to investigate the appressorial turgor pressure of *P. pachyrhizi*. Mature appressoria were placed in sorbitol solutions of increasing concentration, and the frequency of cells undergoing cytorrhysis was recorded for each solution by microscopic inspection (Fig. 3a). Interpolating for the sorbitol solution in which 50% of appressoria had collapsed led to an apparent osmotic pressure in these infection cells of 5.13 MPa. In order to confirm the validity of this method, the turgor pressure of appressoria of *M. oryzae* was assessed as a control. By this method, the turgor pressure in melanized infection cells of this fungus was shown to be 8.19 MPa (Fig. 3b), which perfectly matches the published data (Howard *et al.*, 1991).

Mach–Zehnder double-beam interferometry allows the determination of the mean specific OPD in appressoria of *P. pachyrhizi*

Based on the results of the cytorrhysis assay, the estimated appressorial turgor pressure of *P. pachyrhizi* is comparable with that of *C. graminicola*, which is 5.35 MPa (Bechinger *et al.*, 1999), and well below that of *M. oryzae* (8.19 MPa). However, cytorrhysis experiments are prone to misinterpretations, as high cell wall rigidity may lead to an overestimation of the osmotic potential, and appressorial cell wall rigidity may differ significantly in different species. We therefore used MZM as an independent method to compare appressoria of these fungi. MZM allows direct non-invasive measurement of cellular dry mass using phase shift phenomena, as known from phase contrast or differential interference contrast (DIC) microscopy. An advancement to the basic procedure was achieved in Mach–Zehnder interferometry by aligning two separate parallel beam paths, each with its own condenser and exactly matching objectives. This set-up allowed accurate quantification of the phase shift (OPD) caused by a cell in the object beam path in relation to the reference beam path. The OPD can be visualized by interference band patterns (Fig. S2b) and accurately determined by measuring the displacement of the interference bands. However, objects with inhomogeneous content, such as cells, do not cause an even displacement of the interference bands, and are thus not accurately described by just a single measurement. This is one of the reasons why Mach–Zehnder double-beam interferometry has failed to become a widely applied method in cell biology. The phase shift algorithm developed by Schwider *et al.* (1983) overcomes this problem by using a series of five captured images which differ from each other by a phase shift of $\lambda/4$, resulting in a distance in phase between the first and the last image of one wavelength (Fig. S2b–h). By processing these five images with software developed by Mahlmann *et al.* (2008), a false colour image is created, in which each OPD of $\lambda/2$ is translated into a sequence of colours (colour bar on the bottom right side of Fig. 4b,d). Therefore, objects with OPDs larger than $\lambda/2$ may contain multiple colour sequences (for example, the fully turgid appressorium in Fig. 4b).

As the information on the phase shifts caused by a three-dimensional object is encoded by concentric areas of colour sequences in a two-dimensional image, we introduced a new parameter, that is, the mean specific OPD. The mean specific OPD is no longer related to object size and volume, and consists of the product of the mean OPD and the projection area of the three-dimensional structure divided by the estimated volume of the structure. This value can be easily used to compare structures of wild-type and mutants or, as in our case, to compare appressoria of different species. As the OPD is caused by phase-shifting substances, a higher mean specific OPD value implies a higher concentration of substances, which, in turn, would account for a higher osmotic potential.

So far, we have calculated the mean specific OPD for entire appressoria, that is, a structure containing cell walls and protoplasts (Fig. 4a,b). However, for further assessment of the

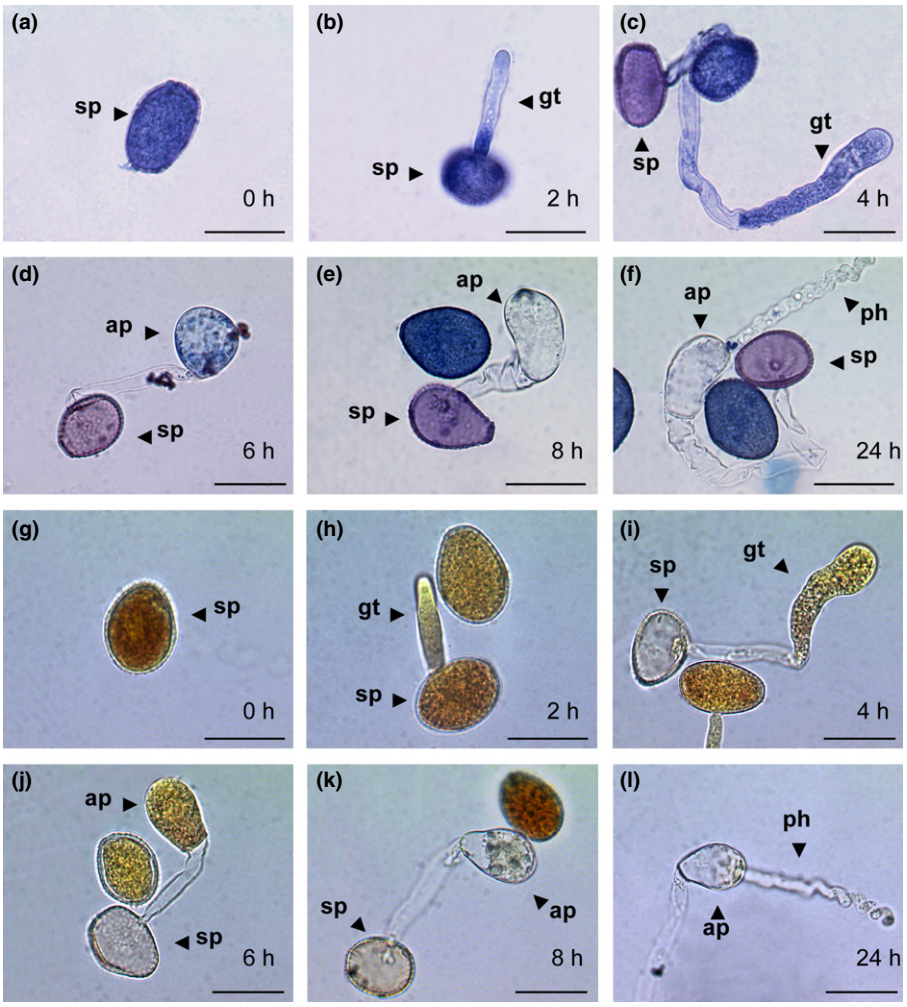

Fig. 2 Glycogen accumulation and degradation in infection structures of *Phakopsora pachyrhizi*. Uredospores were investigated 0–24 h after plating onto glass slides. Representative images of infection structures stained with either haematoxylin solution (a–f) or iodine–potassium iodide solution (g–l) are depicted. ap, appressorium; gt, germ tube; ph, penetration hypha; sp, uredospore. Bars, 20 μm

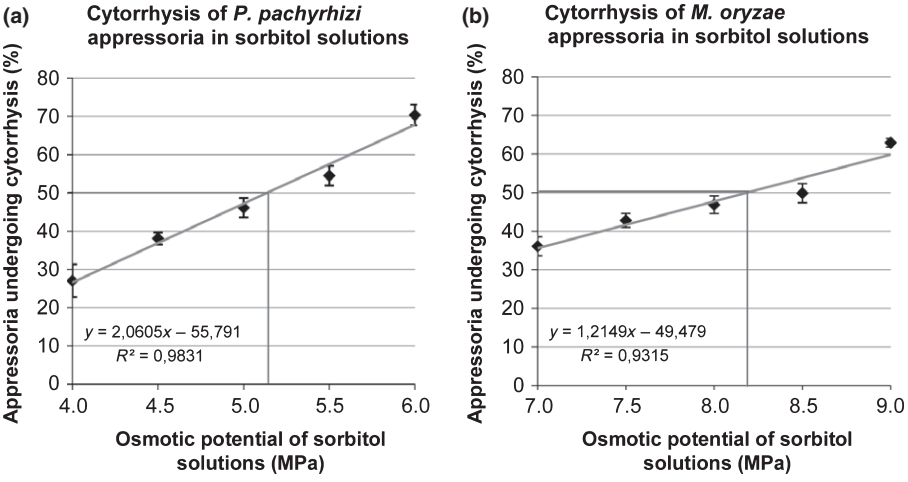

Fig. 3 Investigation of incipient cytorrhysis on appressoria of *Phakopsora pachyrhizi* and *Magnaporthe oryzae*. Appressoria of *P. pachyrhizi* formed on glass slides were incubated in sorbitol solutions of different osmotic potentials (4.0–6.0 MPa) and the proportion of cells that had undergone incipient cytorrhysis was determined microscopically (a). The sorbitol solution in which 50% of appressoria showed cytorrhysis was interpolated. Appressoria of *M. oryzae* were assessed in the same manner using sorbitol solutions of 7.0–9.0 MPa (b). At least 100 appressoria in three independent experiments were investigated. Error bars, ± SD.

appressorial osmotic pressure, we need to know the mean specific OPD separately for protoplasts. This was achieved by determining the difference in the mean specific OPD between entire appressoria and cell walls, with the latter being measured for empty appressoria of *P. pachyrhizi* after the formation of a penetration hypha (Fig. 4c,d). Appressoria of *M. oryzae* were approached in the same manner after the rupture of cell walls by sonication (Fig. S3a–d). A comparison of the values for entire appressoria, cell wall fractions and protoplasts revealed a lower mean specific OPD for fully turgid appressoria of *P. pachyrhizi* when compared with *M. oryzae* (Fig. 5a–c), indicating a lower concentration of solutes. The mean specific OPDs for protoplasts of fully turgid

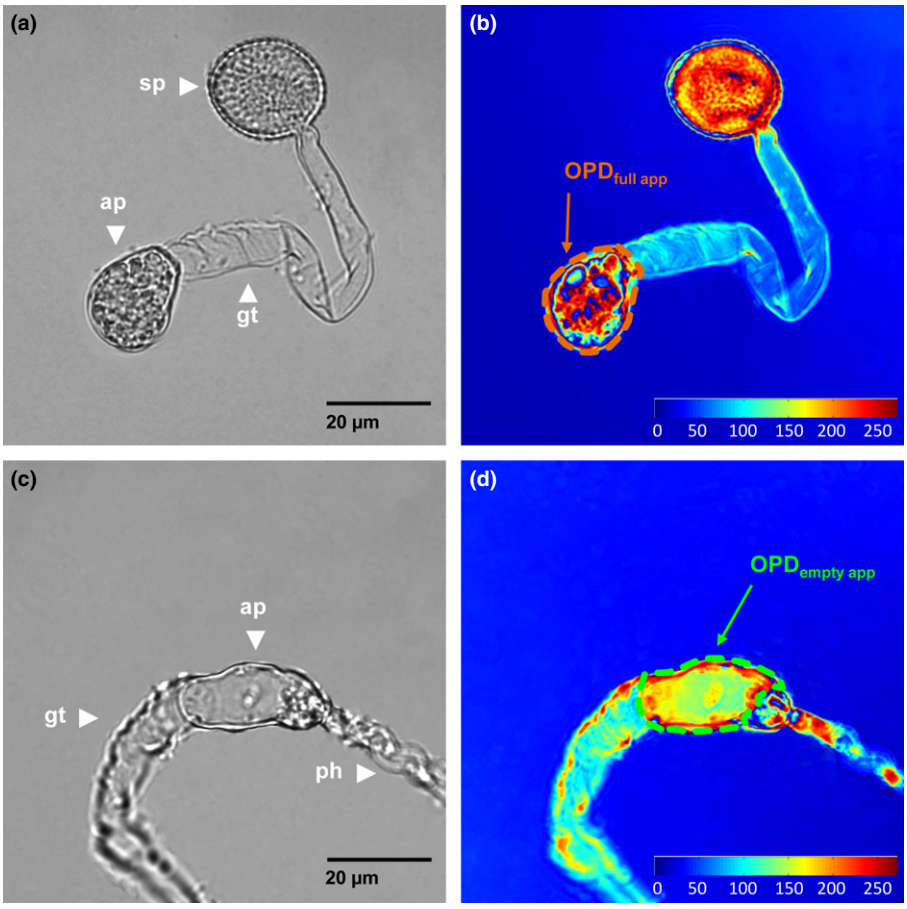

Fig. 4 Infection structures of *Phakopsora pachyrhizi* under transmission light and Mach–Zehnder false colour micrographs. A single uredospore of *P. pachyrhizi*, which had formed an appressorium on glass slides at 8 h after germination, is shown in transmitted light (a). A false colour micrograph of the same appressorium, which was created using the Mach–Zehnder interferometer, is depicted in (b). The latter image consists of five individually captured interference contrast images and was processed with the phase shift algorithm. After the formation of a penetration hypha, an appressorium without cytosolic content could be analysed in the same manner using transmitted light (c) or Mach–Zehnder false colours (d). Each sequence of colours (blue to red, colour bars in the bottom right corners of b and d) represents a phase shift of $\lambda/2$ ($\lambda = 546$ nm). Transmitted light images were taken using differential interference contrast (DIC) optics. Bars, 20 µm. ap, appressorium; gt, germ tube; $OPD_{empty\ app}$, optical path difference of empty appressorium; $OPD_{full\ app}$, optical path difference of full appressorium; ph, penetration hypha; sp, uredospore. For the calculation of OPD, see Supporting Information Table S1a.

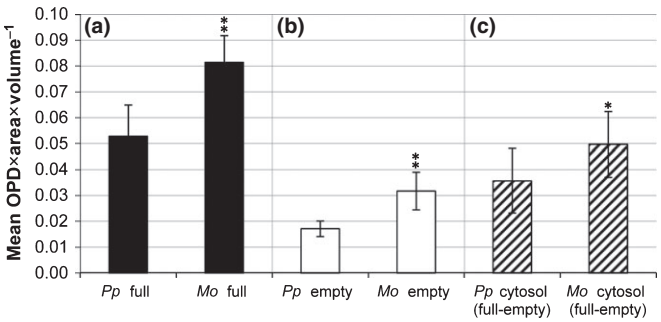

Fig. 5 Comparison of *Phakopsora pachyrhizi* and *Magnaporthe oryzae* appressoria on the basis of their mean specific optical path difference (OPD). The 'mean specific OPD' is calculated by multiplication of the mean OPD (µm) with the area of measurement (µm²) divided by the estimated volume (µm³) of the structure in question. This value was determined for full and empty appressoria. A higher mean specific OPD was found for fully turgid *M. oryzae* appressoria ('*Mo* full') as compared with those of *P. pachyrhizi* ('*Pp* full') (a). The same difference was found for the cell wall component of both pathogens ('*Pp* empty', '*Mo* empty') depicted in (b). Subtraction of the values obtained for full and empty appressoria yielded the mean specific OPD for the cytosolic component of the appressoria (c). The latter was *c.* 26% lower for *P. pachyrhizi* than for *M. oryzae*, indicating a difference in composition and/or concentration of phase shifting substances. Calculations are based on at least 20 measurements for each structure (raw data depicted in Supporting Information Table S2). Error bars, ± SD. Statistical significance was tested by Student's *t*-test: *, $P = 0.01$; **, $P = 0.05$.

appressoria of *P. pachyrhizi* and *M. oryzae* were 0.035 and 0.05, respectively (Fig. 5c).

GC-MS analyses reveal sugar alcohols as predominant osmolytes in appressoria of *P. pachyrhizi*

The use of Mach–Zehnder interferometry allowed accurate measurement of the mean specific OPD of protoplasts. This information was used to answer the question of which osmolytes contribute to the appressorial turgor pressure. For this type of analysis, we had to convert, stepwise, the mean specific OPD: first, into the dry mass of the appressorial content, and next into the osmolyte concentration. The latter could then be used in the van't Hoff equation to calculate the osmotic pressure. For the conversion of OPD into dry mass, the differential index of refraction is needed (refractive index increment, dn/dc), which is a substance-specific value and therefore requires a knowledge of substance composition of the appressoria of *P. pachyrhizi*.

The composition of the content of *P. pachyrhizi* infection structures was analysed in detail by GC-MS, using either re-hydrated uredospores, *in vitro*-germinated uredospores with germ tubes or fractions that had differentiated up to 30% appressoria. Essentially, the distribution of substances in these individual samples did not differ significantly from each other. Therefore, the GC-MS profile of the fraction with appressoria

was used to calculate the relative abundance of substance classes (Fig. S4a). Importantly, in appressoria, and likewise in spores and germ tubes, the C_6-polyol mannitol was identified as the predominant constituent (49%), followed by C_5-polyols, and glucose, glycerol and myo-inositol (Fig. 6a). In samples of *M. oryzae* with up to 40% appressoria, glucose and glycerol represent the most prominent osmolytes, followed by mannitol, C_5-sugar alcohols and myo-inositol (Fig. 6b). This result was surprising, as previous data have suggested that glycerol is the most prominent, if not the only, osmolyte in appressoria of *M. oryzae* (de Jong *et al.*, 1997). It could not be excluded that contaminants from the *M. oryzae* culture medium, for example, glucose, stuck to the spore surface and therefore were included in the GC-MS analysis; however, as a result of extensive washing of the spores after collection from culture plates, this should be negligible.

We further assessed the turgor pressure, following the assumption that the appressorial content only contained the determined sugar alcohols. Accordingly, a mean dn/dc value of the total appressorial content was calculated as the sum of individual dn/dc values of the predominant sugar alcohols rated by their relative abundance (calculation details are given in Table S1b; mean $dn/dc = 0.145\ ml\ g^{-1}$). This dn/dc value, together with the previously determined mean specific OPD, was employed to calculate the concentration of the total dry mass ($c_{dry\ mass}$) of the appressorial protoplast using the equation $c_{dry\ mass} = \text{mean specific OPD}_{protoplast} \times (dn/dc)_{(mean)}^{-1}$ (Table S1c). The concentration of osmolytes ($c_{osmolytes}$) was then calculated by dividing the concentration of the dry mass by the average molecular weight of the appressorial constituents ($M_{(mean)}$, Table S1b). Finally, the osmotic pressure (Π, nomenclature according to Nobel, 2009) of the appressorial protoplast was calculated using the van't Hoff equation ($\Pi = cRT$). By application of this calculation and on the basis of the assumption that the appressorial osmolytes only consist of sugar alcohols, the average osmotic pressure of fully turgid protoplasts of *P. pachyrhizi*, determined by Mach–Zehnder double-beam interference microscopy, equals 3.65 MPa (Table S1c).

For comparison, we determined the osmotic pressure of *M. oryzae* appressoria using the same methodology and performing the required GC-MS analyses to identify the osmolyte content of its appressoria (Fig. S4b). This approach resulted in a calculated osmotic pressure of 6.08 MPa (Table S1c).

Estimation of force exerted during penetration

For successful penetration, appressoria of *P. pachyrhizi* translate turgor pressure into mechanical force, used to breach the plant cuticle and cell wall. The force exerted by a penetration hypha is hard to calculate as the outgrowth of a hypha is a dynamic process, and the exact shape of the hyphal tip is not known and may change during invasive growth. Therefore, we measured the diameter of the penetration pore in successfully invaded cells and, from this, deduced the diameter of the penetration peg, and assumed that the pressure was applied equally over the cross-sectional area. For this approach, barley was utilized as a non-host plant for *P. pachyrhizi*, which is penetrated in the same way as the authentic soybean host (Hoefle *et al.*, 2009; Goellner *et al.*, 2010). Fortunately, barley forms cell wall appositions at the inner epidermal cell wall as a response to penetration by *P. pachyrhizi*, which made it easier to visualize and measure the diameter of the penetration pore. An additional advantage for microscopy is that large epidermal strips can be isolated from barley leaves (Fig. 7). In this way, a pore diameter of 1.2 μm was determined, corresponding to a pore area of 1.1 μm^2 (mean value from 18 measurements). Depending on whether we calculated the physical force exerted by appressoria of *P. pachyrhizi* on the basis of turgor pressure determined by MZM, or incipient cytorrhysis, it equals 3.9 or 5.5 μN.

As a control, we calculated the force exerted by the melanized appressorium of *M. oryzae*. The diameter of the penetration pore

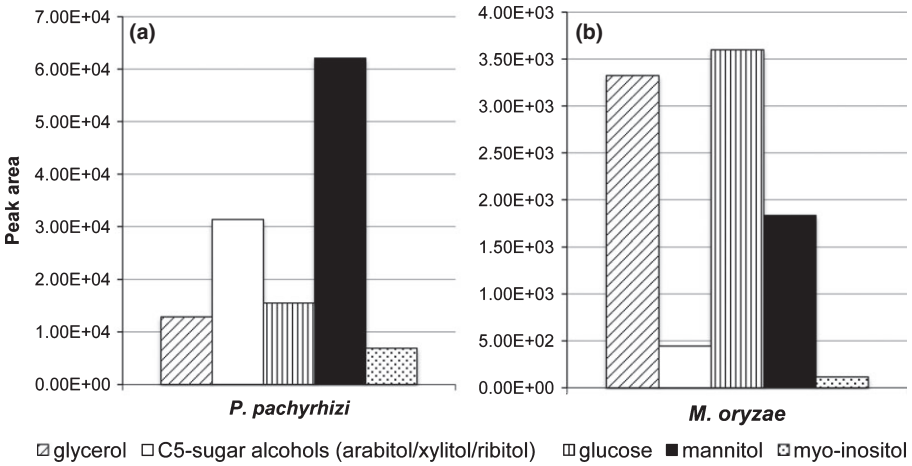

Fig. 6 Relative amounts of the most abundant osmolytes in the cytosol of *Phakopsora pachyrhizi* and *Magnaporthe oryzae* as measured by GC-MS. Spores of *P. pachyrhizi* (15 mg) and *M. oryzae* (1.2×10^6 spores) were germinated in water or on glass slides until appressoria had been formed, and then processed for GC-MS analyses. The peak areas of the five most abundant substances, glycerol, glucose, C_5-polyols (mainly arabitol but also small amounts of xylitol and ribitol), C_6-polyols (mainly mannitol and marginal amounts of sorbitol and galactitol) and myo-inositol, are summarized in (a) and (b). Representative results of single experiments from three biological replicates for *P. pachyrhizi* and two replicates for *M. oryzae* are shown. Detailed chromatograms are shown in Supporting Information Fig. S4.

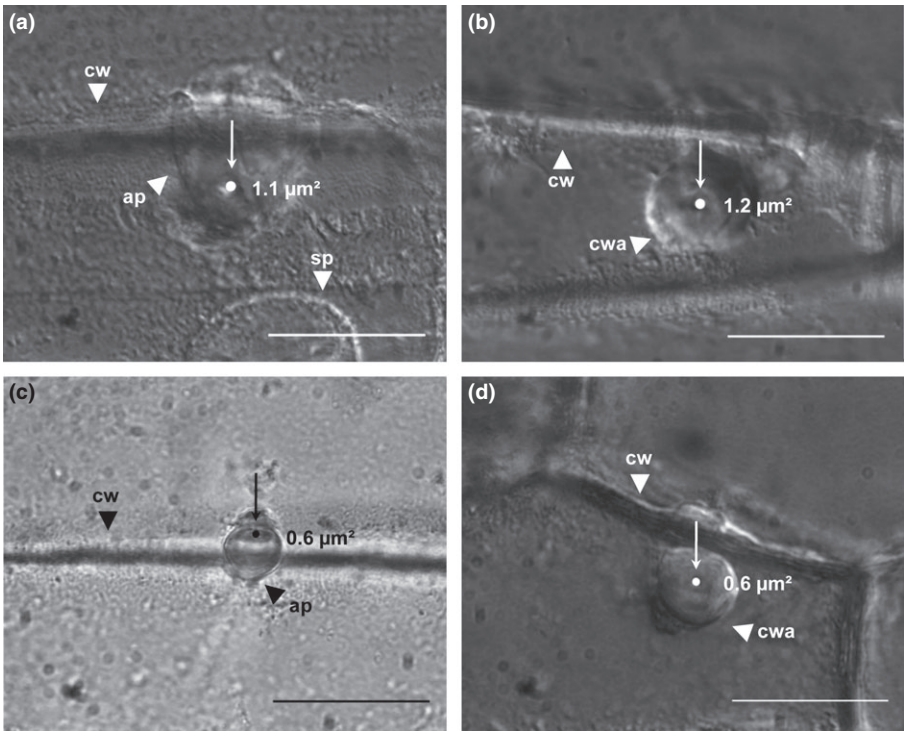

Fig. 7 Measurement of penetration holes caused by hyphae of *Phakopsora pachyrhizi* and *Magnaporthe oryzae*. Abaxial surfaces of primary leaves of 7-d-old barley plants were inoculated with *P. pachyrhizi* and *M. oryzae* spore suspensions. Epidermal tissue was peeled at 48 h post-inoculation (hpi) and placed onto microscope slides. Cross-sectional areas (marked by arrows) of penetration holes caused by *P. pachyrhizi* (a) and *M. oryzae* (c) were measured at the inner side of the epidermal peel. Papillae successfully penetrated by *P. pachyrhizi* (b) and *M. oryzae* (d) were also used for measurements. Representative images are shown from 18 and 21 measurements for *P. pachyrhizi* and *M. oryzae*, respectively. Images were taken at ×1000 magnification using differential interference contrast (DIC) optics. ap, appressorium; cw, cell wall; cwa, cell wall apposition; sp, spore. Bars, 20 µm.

of *M. oryzae* was 1.1 µm and the deduced area was 0.9 μm^2 (mean value from 21 measurements), which corresponded to a force of 5.9 µN (MZM) or 7.2 µN (incipient cytorrhysis). Interestingly, the penetration force exerted by both fungi was approximately the same. In order to demonstrate the enormous force generated by a non-melanized appressorium, we examined whether *P. pachyrhizi* and *M. oryzae* differ in their capability to penetrate non-biodegradable artificial membranes. We used PTFE-like membranes of highly defined thickness because they are known to simulate the cuticle and epidermal cell wall with respect to hydrophobicity and penetration resistance (Kuster *et al.*, 2008). Surprisingly, *P. pachyrhizi* was able to penetrate all membranes, even those with the highest thickness of 130 µm (Table 1). By contrast, *M. oryzae*, which formed appressoria only on 130-nm-thick membranes, was unable to penetrate, suggesting that non-melanized appressoria of *P. pachyrhizi* are even more powerful than the melanized appressoria of *M. oryzae*. To further validate this result, and because *M. oryzae* did not form appressoria on 70- and 100-nm-thick membranes, we co-inoculated *C. graminicola*, a fungus that is also known to generate high turgor in its melanized appressoria, onto the same membranes. *Colletotrichum graminicola* formed appressoria on all membranes, but was only able to consistently penetrate the 70-nm membrane, thereby confirming the result for the hyaline appressoria of *P. pachyrhizi* in this assay.

Table 1 Penetration of polytetrafluoroethylene (PTFE) membranes by *Phakopsora pachyrhizi*, *Magnaporthe oryzae* and *Colletotrichum graminicola*

Thickness of membrane (nm)	Penetration success (%)		
	P. pachyrhizi[a]	*M. oryzae*[b]	*C. graminicola*[c]
70	29.98	na	19.70
100	22.78	na	(1)[d]
130	6.95	0	0

Membranes of various thicknesses were simultaneously inoculated with conidia of *P. pachyrhizi*, *M. oryzae* and *C. graminicola*. Membranes were floated on distilled water and incubated for 24 h until appressoria had formed. Penetration success was monitored using a microscope with bright field optics. na, not applicable.

[a]*Phakopsora pachyrhizi* formed appressoria on all membranes. Mean values of *P. pachyrhizi* penetration success on membranes were calculated from four independent experiments each. In total, 1413 appressoria were analysed.

[b]*Magnaporthe oryzae* produced appressoria only on the 130-nm membrane. Successful penetration from these appressoria ($n = 38$) was never observed.

[c]*Colletotrichum graminicola* formed appressoria on all membranes. Mean values are given from four independent experiments for the 70- and 100-nm membranes. The result shown for the 130-nm membrane was obtained in a single experiment which revealed no penetration event among the 101 appressoria inspected.

[d]In four independent experiments ($n = 271$), only a single penetration event '(1)' was found for *C. graminicola* on the 100-nm membranes.

Discussion

The most detailed information on the sequential steps during the appressorial penetration of *P. pachyrhizi* has so far been gained by transmission electron microscopy (Koch *et al.*, 1983; Edwards & Bonde, 2011). The observation that the cuticle is deformed by the penetration peg suggests that mechanical pressure is a main driving force during initial invasion (Edwards & Bonde, 2011). As a result of the absence of signs of deformation in epidermal

cell walls, it was reasoned that, at later stages of penetration, digestive enzymes may also play a role. However, experimental data for the mechanical force applied by appressoria of *P. pachyrhizi* is still lacking. This is mainly a result of methodological problems which, notwithstanding its biological relevance, makes the precise measurement of the mechanical force exerted by plant or hyphal cells difficult (Geitmann, 2006).

Initially, we estimated the appressorial turgor pressure by observing cytorrhysis, which yielded values of 5.13 and 8.19 MPa for *P. pachyrhizi* and *M. oryzae*, respectively (Fig. 3). Although the latter is in almost perfect agreement with the pressure determined by Howard *et al.* (1991), the high value for *P. pachyrhizi* was surprising, particularly as it differentiates non-melanized appressoria. In general, melanization has been demonstrated to be an important virulence factor for many plant pathogenic fungi, including *M. oryzae* (Jacobson, 2000). Inhibition of the melanin biosynthetic pathway, either by application of the fungicide Tricyclazole, which inhibits the reduction of 1,3,8-trihydroxynaphthalene to vermelone (Wheeler, 1982), or genetic manipulation rendered *M. oryzae* avirulent to its host plants (for a review, see Howard & Valent, 1996). Howard *et al.* (1991) proposed that a lack of melanization made *M. oryzae* appressoria more permeable for larger sized osmolytes, and speculated that melanin minimizes pore sizes in appressorial cell walls, and thereby prevents osmolyte leakage which otherwise would stall turgor generation. Results obtained from our GC-MS analyses revealed that mannitol and C_5-sugar alcohols were enriched in appressoria of *P. pachyrhizi*, whereas the smaller sized glycerol seems to play a less important role (Fig. 6). The fact that sorbitol, a stereoisomer of mannitol, which was used in our study as an external osmolyte, caused cytorrhysis rather than plasmolysis on appressoria of *P. pachyrhizi* demonstrated that this solute cannot pass freely through its cell walls. Therefore, their pore size must be < 0.372 nm, which is the radius of gyration for sorbitol molecules (Grigera, 1988). Interestingly, appressoria of *Blumeria graminis* f.sp. *hordei* (*Bgh*), which are also hyaline, are permeable to sorbitol (Pryce-Jones *et al.*, 1999). Our experiments indicate that *P. pachyrhizi* might have evolved structural components other than melanin in appressorial cell walls to prevent osmolyte leakage. The dispensability of melanin in fungal appressoria for turgor generation was recently confirmed in a different study, showing that the turgor in non-melanized appressoria of *C. graminicola* mutants did not differ from that in wild-type melanized appressoria (Ludwig *et al.*, 2013). Our GC-MS analyses revealed glycerol and glucose to be present at equal levels in appressoria of *M. oryzae* (Fig. 6), which is novel, as previous publications postulate glycerol to be the exclusive osmolyte (de Jong *et al.*, 1997). Although unlikely, the high abundance of glucose could conceivably be a result of inadequate washing of the fungal material. In addition, it must be considered that fungal material enriched with appressoria and used for GC-MS profiling was harvested at a fixed time point (8 h), and it cannot be excluded that the appressorial content might change thereafter until penetration takes place.

With the present work, we add an additional technique to the tool box for turgor measurements, namely the application of microscope interferometry. Essentially, interferometer microscopy can be employed to measure the mass of substances dissolved in water within a cell, because of the increase in the refractive index they cause (Davies, 1958). A knowledge of the composition of solutes within a cell, their molecular mass and the cell volume makes it possible to calculate the osmotic potential in that cell. Today, the use of interference microscopy appears to be extraordinary, but only a few decades ago this technique was at the forefront of live cell imaging (Dunn, 1998). Unfortunately, the potential was neglected because computer-aided image analysis had not been developed. We have interfaced one of the old interference microscopes to a computer (Fig. 1a) (Mahlmann *et al.*, 2008). This set-up, together with the phase shift algorithm, allowed the determination of the dry mass of single cells with high accuracy. The latter is possible because cellular material, either dissolved or in the solid state, increases the refractive index in direct proportion (Dunn, 1998). As the refractive index increments (dn/dc) – concentration of a substance that causes an increase in the refractive index by 1% – of biological material, for example, lipids, proteins and nucleic acids, are sufficiently similar to each other (Table S2), several researchers have ignored these minor differences and have made calculations with a mean dn/dc for living cells (Dunn, 1998). As we aimed to be as precise as possible in the measurement of the osmolyte concentration, we applied GC-MS analysis to determine the composition of substances in appressoria. Using this information, we calculated the accurate dn/dc value for the determined appressorial constituents of *P. pachyrhizi*, which was $0.145\ ml\ g^{-1}$ (Table S1b). Interestingly, the dn/dc value determined for *M. oryzae* ($0.135\ ml\ g^{-1}$, Table S1b) is in the same range as the dn/dc value of the appressoria of *P. pachyrhizi*, although their constituents differ significantly from each other (Fig. 6). In addition, the GC-MS data presented here confirm the unpublished NMR data of R. Howard and M. Ferrari (in Howard & Valent, 1996) by showing that substantial amounts of sugar alcohols (mannitol and C_5-sugar alcohols) are also present in appressoria of *M. oryzae* in addition to the usually mentioned glycerol. Taken together, our results demonstrate the considerable differences between accurate dn/dc values, confirmed by GC-MS analyses, and the use of a general dn/dc value for living cells ($0.17\ ml\ g^{-1}$, Table S2) (Mahlmann *et al.*, 2008). A straightforward alternative in comparative experiments, circumventing the need for cell content determination, could be the use of the mean specific OPD.

In this study, we first determined the composition of the appressorial cell content and subsequently used the MZM-measured mean specific OPD values to deduce the resulting osmotic potentials. Accordingly, sugar alcohols were identified as the predominant osmolytes within these cells, and osmotic potentials of 3.65 and 6.08 MPa were calculated for *P. pachyrhizi* and *M. oryzae*, respectively. The values determined for turgor pressure in the appressoria of both fungi by incipient cytorrhysis are greater than those obtained by MZM. However, this was not unexpected, as cytorrhysis tends to over-estimate Ψ_Π owing to the extra energy needed to deform the cell wall (Howard & Valent, 1996). If one gives the cytorrhysis data more credence,

however, another explanation might be that the sugar alcohols only account for *c.* 75% of the overall appressorial turgor pressure and the remaining 25% is contributed by other cell constituents, such as, for example, ions. By measuring the diameter of the penetration pore formed by *P. pachyrhizi* on barley epidermal tissue and based on the MZM-measured turgor pressure, we deduced that a mechanical force of 3.9 μN is exerted by the penetration hypha. Similarly, a mechanical force of 5.9 μN was calculated for the penetration peg of *M. oryzae*, which is higher than the mechanical force exerted by *P. pachyrhizi*. However, *P. pachyrhizi*, but not *M. oryzae*, is able to penetrate thick artificial membranes. Therefore, it must be concluded that other characteristics, for example, the shape or rigidity of penetration hyphae, may also add to the efficiency of this process.

Although ASR is economically highly important and much effort has been made to combat the disease, so far little attention has been paid to the penetration process itself. Our studies revealing the unexpectedly high penetration force exerted by appressoria of *P. pachyrhizi* suggest that this process could be a promising novel target for future plant protection strategies, for example, by creating fungicides that interfere with the synthesis of osmolytes or increase osmolyte leakage from appressoria. The application of Mach–Zehnder interferometry to the appressoria of fungi other than *P. pachyrhizi* and *M. oryzae* will aid in the understanding of the role of elevated turgor pressure for penetration success of plant pathogenic fungi on a broader scale.

Acknowledgements

M.L. was supported by a grant from the RWTH Aachen University within the framework of the graduate programme. The authors are grateful to A. J. Slusarenko for helpful discussions and critical reading of the manuscript.

References

Bechinger C, Giebel KF, Schnell M, Leiderer P, Deising HB, Bastmeyer M. 1999. Optical measurements of invasive forces exerted by appressoria of a plant pathogenic fungus. *Science* **285**: 1896–1899.

Bromfield KR. 1984. *Soybean rust*. St Paul, MN, USA: American Phytopathological Society.

Davies H. 1958. The determination of mass and concentration by microscope in interferometry. *General Cytochemical Methods* **1**: 55–161.

Deising HB, Werner S, Wernitz M. 2000. The role of fungal appressoria in plant infection. *Microbes and Infection* **2**: 1631–1641.

Dunn GA. 1998. Transmitted-light interference microscopy: a technique born before its time. *Proceedings of the Royal Microscopical Society* **33**: 189–196.

Edwards HH, Bonde MR. 2011. Penetration and establishment of *Phakopsora pachyrhizi* in soybean leaves as observed by transmission electron microscopy. *Phytopathology* **101**: 894–900.

Freytag S, Bruscaglioni L, Gold RE, Mendgen K. 1988. Basidiospores of rust fungi (*Uromyces species*) differentiate infection structures *in vitro*. *Experimental Mycology* **12**: 275–283.

Geitmann A. 2006. Experimental approaches used to quantify physical parameters at cellular and subcellular levels. *American Journal of Botany* **93**: 1380–1390.

Goellner K, Loehrer M, Langenbach C, Conrath U, Koch E, Schaffrath U. 2010. *Phakopsora pachyrhizi*, the causal agent of Asian soybean rust. *Molecular Plant Pathology* **11**: 169–177.

Grigera JR. 1988. Conformation of polyols in water. Molecular-dynamics simulation of mannitol and sorbitol. *Journal of the Chemical Society, Faraday Transactions 1: Physical Chemistry in Condensed Phases* **84**: 2603–2608.

Hoefle C, Loehrer M, Schaffrath U, Frank M, Schultheiss H, Hueckelhoven R. 2009. Transgenic suppression of cell death limits penetration success of the soybean rust fungus *Phakopsora pachyrhizi* into epidermal cells of barley. *Phytopathology* **99**: 220–226.

Horobin R, Murgatroyd L. 1971. The staining of glycogen with Best's Carmine and similar hydrogen bonding dyes. A mechanistic study. *Histochemical Journal* **3**: 1–9.

Howard RJ, Ferrari MA, Roach DH, Money NP. 1991. Penetration of hard substrates by a fungus employing enormous turgor pressures. *Proceedings of the National Academy of Sciences, USA* **88**: 11281–11284.

Howard RJ, Valent B. 1996. Breaking and entering: host penetration by the fungal rice blast pathogen *Magnaporthe grisea*. *Annual Review of Microbiology* **50**: 491–512.

Hummel J, Strehmel N, Selbig J, Walther D, Kopka J. 2010. Decision tree supported substructure prediction of metabolites from GC-MS profiles. *Metabolomics* **6**: 322–333.

Jacobson ES. 2000. Pathogenic roles for fungal melanins. *Clinical Microbiology Reviews* **13**: 708–717.

Jahnke J, Mahlmann DM, Jacobs P, Priefer UB. 2011. The influence of growth conditions on the cell dry weight per unit biovolume of *Klebsormidium flaccidum* (Charophyta), a typical ubiquitous soil alga. *Journal of Applied Phycology* **23**: 655–664.

de Jong JC, McCormack BJ, Smirnoff N, Talbot NJ. 1997. Glycerol generates turgor in rice blast. *Nature* **389**: 244–245.

Koch E, Ebrahimnesbat F, Hoppe HH. 1983. Light and electron-microscopic studies on the development of soybean rust (*Phakopsora pachyrhizi* Syd) in susceptible soybean leaves. *Phytopathologische Zeitschrift* **106**: 302–320.

Koch E, Hoppe HH. 1988. Development of infection structures by the direct-penetrating soybean rust fungus (*Phakopsora pachyrhizi* Syd) on artificial membranes. *Journal of Phytopathology-Phytopathologische Zeitschrift* **122**: 232–244.

Kuster S, Ludwig N, Willers G, Hoffmann J, Deising HB, Kiesow A. 2008. Thin PTFE-like membranes allow characterizing germination and mechanical penetration competence of pathogenic fungi. *Acta Biomaterialia* **4**: 1809–1818.

Langenbach C, Campe R, Schaffrath U, Goellner K, Conrath U. 2013. UDP-glucosyltransferase UGT84A2/BRT1 is required for Arabidopsis nonhost resistance to the Asian soybean rust pathogen *Phakopsora pachyrhizi*. *New Phytologist* **198**: 536–545.

Latgé J-P. 2007. The cell wall: a carbohydrate armour for the fungal cell. *Molecular Microbiology* **66**: 279–290.

Lew RR. 2011. How does a hypha grow? The biophysics of pressurized growth in fungi. *Nature Reviews Microbiology* **9**: 509–518.

Loehrer M, Langenbach C, Goellner K, Conrath U, Schaffrath U. 2008. Characterization of nonhost resistance of Arabidopsis to the Asian soybean rust. *Molecular Plant–Microbe Interactions* **21**: 1421–1430.

Loehrer M, Schaffrath U 2011. Asian soybean rust – meet a prominent challenge in soybean cultivation. In: Ng T-B, ed. *Soybean – biochemistry, chemistry and physiology*. Rijeka, Croatia: InTech, 83–100. doi: 10.5772/15651.

Ludwig N, Loehrer M, Hempel M, Mathea S, Schliebner I, Menzel M, Kiesow A, Schaffrath U, Deising HB, Horbach R. 2013. Melanin is not required for turgor generation but enhances cell wall rigidity in appressoria of the corn pathogen *Colletotrichum graminicola*. *Molecular Plant–Microbe Interactions* **27**: 315–327.

Mahlmann DM, Jahnke J, Loosen P. 2008. Rapid determination of the dry weight of single, living cyanobacterial cells using the Mach–Zehnder double-beam interference microscope. *European Journal of Phycology* **43**: 355–364.

Money NP. 2004. The fungal dining habit: a biomechanical perspective. *Mycologist* **18**: 71–76.

Nobel PS. 2009. *Physicochemical and environmental plant physiology*. Oxford, UK: Elsevier Academic Press.

Pryce-Jones E, Carver T, Gurr SJ. 1999. The roles of cellulase enzymes and mechanical force in host penetration by *Erysiphe graminis* f.sp *hordei*. *Physiological and Molecular Plant Pathology* **55**: 175–182.

Schwider J, Burow R, Elssner KE, Grzanna J, Spolaczyk R, Merkel K. 1983. Digital wave-front measuring interferometry: some systematic error sources. *Applied Optics* **22**: 3421–3432.

Thines E, Weber RWS, Talbot NJ. 2000. MAP kinase and protein kinase A-dependent mobilization of triacylglycerol and glycogen during appressorium turgor generation by *Magnaporthe grisea*. *Plant Cell* **12**: 1703–1718.

Uppalapati SR, Ishiga Y, Doraiswamy V, Bedair M, Mittal S, Chen J, Nakashima J, Tang Y, Tadege M, Ratet P *et al.* 2012. Loss of abaxial leaf epicuticular wax in *Medicago truncatula irg1/palm1* mutants results in reduced spore differentiation of anthracnose and nonhost rust pathogens. *Plant Cell* **24**: 353–370.

Wheeler MH. 1982. Melanin biosynthesis in *Verticillium dahliae*: dehydration and reduction reactions in cell-free homogenates. *Experimental Mycology* **6**: 171–179.

Zellerhoff N, Himmelbach A, Dong W, Bieri S, Schaffrath U, Schweizer P. 2010. Nonhost resistance of barley to different fungal pathogens is associated with largely distinct, quantitative transcriptional responses. *Plant Physiology* **152**: 2053–2066.

Supporting Information

Additional supporting information may be found in the online version of this article.

Fig. S1 Comparison of infection structures formed by *Phakopsora pachyrhizi* on glass slides (*in vitro*) and soybean leaves (*in vivo*).

Fig. S2 Visualization and measurement of the optical path difference (OPD) by displacement of interference band patterns using a Mach–Zehnder double-beam interferometer.

Fig. S3 Fully turgid and empty appressoria of *Magnaporthe oryzae* imaged in bright field and Mach–Zehnder microscopy.

Fig. S4 GC-MS profiles of soluble material in fractions enriched with appressoria from *Phakopsora pachyrhizi* and *Magnaporthe oryzae*.

Table S1 Calculation details for the determination of the turgor pressure in appressoria of *Phakopsora pachyrhizi* and *Magnaporthe oryzae*

Table S2 Overview of the specific refractive index increment for different biological osmolytes

Please note: Wiley Blackwell are not responsible for the content or functionality of any supporting information supplied by the authors. Any queries (other than missing material) should be directed to the *New Phytologist* Central Office.